ISSN 1027-4510, Journal of Surface Investigation. X-ray, Synchrotron and Neutron Techniques, 2014, Vol. 8, No. 5, pp. 1082–1088. © Pleiades Publishing, Ltd., 2014.

Compaction of a Copper Film on Graphene by Argon-Beam Bombardment: Computer Experiment

A. E. Galashev[a] and V. A. Polukhin[b]

[a] *Institute of Industrial Ecology, Ural Branch, Russian Academy of Sciences, Yekaterinburg, 620219 Russia*
e-mail: galashev@ecko.uran.ru

[b] *Institute of Material Studies and Metallurgy, Ural Federal University, Yekaterinburg, 620002 Russia*

Received October 29, 2013

Abstract—The process of Cu-film compaction on graphene under the action of Ar_{13} clusters hitting the surface with an energy of 5 eV is studied using the molecular-dynamics method. The horizontal and vertical components of the self-diffusion coefficient of a Cu film and graphene, the stresses on the horizontal Cu area, the Cu–graphene interaction energy, the radial distribution function of the film, and the graphene surface roughness under bombardment of a target by Ar_{13} clusters are calculated. Graphene exhibits some pliability, and traces of Cu film surface relief remain on it after total exposure under the impacts of Ar_{13} clusters.

DOI: 10.1134/S1027451014050279

INTRODUCTION

It is well-known that 6-keV Ar-ion beams decrease steel surface roughness at normal incidence (the incident angle θ is 0°), while they increase the roughness at rather oblique incidence (θ = 85°–87°) [1]. Ar beams with higher energies (50–150 keV) are used to modify the surface of hydrocarbon steel with implanted nitrogen [2]. As a result of such treatment, fine nitride inclusions become consolidated and large inclusions are crushed.

After sample treatment by a high-energy ion beam, the bulk structure can contain a "template", which was present on the original surface. After bombardment, the approximate pattern of metal-structure transformation includes ions incident on the metal surface, penetrating into it, and hitting neighboring atoms as billiard balls. This process occurring at the atomic level is close to melting. But it differs from ordinary melting, because atoms participating in it more closely resemble magnetic billiard balls, since they form clusters around them. Groups of displaced atoms, which glide back toward the surface, form in the crystal lattice. They return as a group and consolidate their positions again, but in a different order. As the distance from the surface increases, the structure also changes. Here some atoms move from their places. As a result, vacancies form in the crystal lattice (not far from the surface). On the other hand, a layer with a larger stress appears; here, atoms are located near to each other and far from rarified space. There is excess compression in this accumulation of atoms. We can say that two layers with different compression and stretching levels are produced in the metal. The formation of a double layer is often a precursor of the gliding mode. The presented pattern of structure variations in the metal can change strongly if a very thin metal film is the target for bombardment.

Using low-energy ions (1 keV or less) is the most promising way of decreasing surface distortions. Mechanical polishing of polycrystalline copper under bombardment with an oblique 1-keV Ar-ion beam (with a θ angle of 70°) was performed in [3]. The results showed that oblique ion bombardment is useful in decreasing the heights and the number of asperities on the surface.

Using cluster beams looks encouraging. In this case, the increase in the cluster energy is a multiple of the number of atoms in the cluster at the same velocity, and it is thus possible to avoid large optical aberrations in focusing systems. A 10-keV cluster ion beam with an average size of 2000 Ar atoms turned out to be sufficient to decrease the average surface roughness of indium and tin oxide on a substrate to approximately one-quarter of the initial value [4]. In prospect, using cluster beams will make it possible to create a series of radically new technologies for cleaning surfaces and develop a new generation of ion sources. At the same time, the physical model of sputtering under cluster bombardment has not been developed yet to a level that would make it possible to obtain reliable quantitative estimates of the observed effects.

Treatment with an ion beam is one of the most effective compaction methods. The mechanism for compacting a Cu film on graphene can be studied in detail using a computer experiment. Our study showed that the 10 eV Ar cluster bombardment of the Cu film on graphene at θ angle of 0° leads finally to complete cleaning of the graphene sheet of copper.

The aim of the present paper is to study the structure and the kinetic and mechanical properties of a Cu film on graphene compacted by a 5-eV Ar beam.

COMPUTER MODEL

Compaction of the structure of a Cu film on graphene by 5-eV Ar beams was simulated using the method of molecular dynamics (MD). The graphene consisted of 406 carbon atoms embedded in a two-dimensional hexagonal lattice in the form of a rectangular sheet with a size of 3.8×3.2 nm. The interaction between C atoms was described by the multiparticle Tersoff potential [5] with the covalent-bonding distance increased to 0.23 nm and with the inclusion of additional weak attraction for $r > 0.23$ nm which was specified by the Lenard-Jones potential with the parameters obtained in [6]. To eliminate the resulting rotational moment in each node of the graphene sheet, the rotational component of the force created by atoms of adjacent nodes was excluded. The analytic form of the local rotational moment of the interaction potential was given in [6]. The interaction between the Cu atoms was described by the multiparticle Sutton–Chen potential whose analytical form and parameters were given in [7]. The details of the application of multiparticle potentials for the simulation of C–C and Cu–Cu interactions and the method for calculating stresses in the metal film were given in [8]. The interaction between C and Cu atoms was represented in the form of the Morse potential with the parameters determined in [9].

Obtaining a stable metal film on graphene first suggests attaining a high degree of adhesion of the metal to the substrate (graphene). This can be attained if the metal atoms closely approach C atoms, occupying energetically advantageous places on the graphene surface. Hexagonal cells formed by C atoms are such places. It is energetically advantageous to place metal atoms centrally symmetrically above the hexagonal cells [10]. In this case, the distance from the metal atom to the graphene plane is determined either experimentally or by means of quantum-mechanical calculations. The problem of such filling of graphene with metal atoms consists in the mismatch between the lattice periods of the metal crystal and graphene. Because the graphene lattice period is significantly smaller than that of the metal, the hexagonal cells must be ignored when filling graphene with the metal in each of the two dimensions. For copper, alternate cells in both directions can be filled. For such filling, only 49 Cu atoms are located on the graphene sheet consisting of 406 C atoms. When metal atoms are deposited, nonadjacent graphene cells are filled at times that are hard to obtain in the MD calculation. Therefore, the first stage of deposition consisted of the forced arrangement of 49 Cu atoms in energetically most advantageous positions on the graphene sheet. Cu atoms were advanced a distance of 2.243 Å (calculated in accordance with density functional theory [11]) to C atoms. Because of the long-range character of the interaction between Cu atoms, these Cu atoms deposited on the graphene surface served as a basis for further growth of the metal film from the material approaching the surface. The second stage of deposition consisted of the random dropping of 51 Cu atoms over the graphene sheet containing 49 already deposited metal atoms. The atoms were dropped in a rectangular parallelepiped with a base reproducing the graphene sheet and a height of $2\sigma_{Cu-C}$, where $\sigma_{Cu-C} = 0.3225$ nm [12] is the Lenard-Jones parameter describing the Cu–C interaction. The distance from the lower parallelepiped base to the plane passing through the centers of mass of C atoms was $3\sigma_{Cu-C}$. In addition to the usual thermal velocities (corresponding to a temperature of 300 K), the vertically downward-directed component of the velocity v_{mp}, where $v_{mp} = \sqrt{2kT/m}$ is the most probable velocity in the Maxwell distribution, was added to the randomly scattered Cu atoms at the initial instant of time. A Cu atom with such a velocity could pass a distance of σ_{Cu-C} in vacuum in a period of 16.3 ps. As the deposited Cu atom moved a distance of $1.1\ \sigma_{Cu-C}$ or less toward the C atoms or preliminary deposited Cu atoms, the additional vertical component was subtracted from its velocity. Thus, a relatively stable Cu film on graphene formed during a time period with a duration of $10^6\ \Delta t$ ($\Delta t = 0.2$ fs) or 200 ps. Such a time step was further used in the simulation with the ion beam.

The surface was bombarded by ion beams in accordance with the following scheme. A virtual rectangular two-dimensional mesh with a division of 5×5 was superimposed on the graphene sheet. The mesh nodes were distributed uniformly over the sheet surface at a distance of σ_{Cu-C} from the edges. The virtual mesh was raised above the graphene sheet to a distance of 1.5 nm. An Ar_{13} cluster center was placed at each mesh node in turn at equal time intervals of $\tau = 16$ ps. In other words, each mesh node specified the initial position of the Ar_{13} cluster with a lifetime of 16 ps, which interacted with the target in this time. At the initial time instant, all Ar_{13} cluster atoms acquired the same velocities directed downward and corresponding to a kinetic energy of 5 eV. For such a velocity, the Ar atom travels the distance σ_{Cu-C} in 6.5 ps. After the collision, a fraction of Ar atoms was scattered in different directions, and a fraction penetrated into the loose metal packing, where it continued to interact with copper and graphene. After a period of 16 ps, Ar atoms of the destroyed cluster were removed from the system, and a new Ar_{13} cluster was ready to bombard the substrate. The interaction between atoms in the Ar_{13} cluster was described by the Lenard-Jones potential with parameters of $\sigma_{Ar-Ar} = 0.3405$ nm and $\varepsilon_{Ar-Ar} = 0.0103$ eV [13].

The interaction between the Ar atoms and target atoms (Cu and C) was given by the Moliére potential [14]:

$$\Phi = Z_i Z_j \frac{e^2}{r} M\left\{0.35\exp\left(-0.3\frac{r}{a}\right) + 0.55\exp\left(-1.2\frac{r}{a}\right) + 0.10\exp\left(-6.0\frac{r}{a}\right)\right\}. \quad (1)$$

Here, Z_i and Z_j are the atomic numbers i and j, e is the elementary electric charge, r is the distance between atoms, and a is the Firsov screening length [15]:

$$a = 0.885 a_0 (Z_i^{1/2} + Z_j^{1/2})^{-2/3}, \quad (2)$$

where a_0 is the Bohr radius. The attracting interaction between the Ar and C atoms and between Ar and Cu is small, and it can be neglected, because the primary aim of this study is the energy and angular momentum transfer rather than the chemical bonding [16].

It was assumed that the Ar ions hit the surface as neutral atoms with the same energy as the initial ion. If bombardment was performed with charged atoms, then the ion charge must be neutralized on the surface by the charge exchange. However, the electron moves faster than the nucleus by at least three orders of magnitude. Therefore, the dynamics of the Ar ion is similar to that of a neutral Ar atom within the limits of the Oppenheimer approximation [17, 18]. The charge cannot accumulate under target bombardment, because each charge carried by the ion is always neutralized upon impact on the target. Numerical integration of the equations of motion was carried out using the fourth-order Runge–Kutta scheme [19]. Four series of target bombardment with Ar clusters with the same durations (400 ps) were performed. Each cluster impact on the surface led to system heating. The heat released from the system was removed effectively in accordance with the Berendsen scheme with the bonding constant $\tau = 4$ fs [20]. To control temperature, at each time step, the velocities v were scaled in accordance with

$$v = \lambda v, \quad \lambda = \left[1 + \frac{\Delta t}{\tau}\left(\frac{T_0}{T} - 1\right)\right]^{1/2}, \quad (3)$$

where λ is the scaling factor, T_0 is the given temperature (300 K), and T is the current temperature.

The self-diffusion coefficient is expressed in terms of the average squared atomic displacement $\langle \Delta \mathbf{r}(t)]^2 \rangle$ [21]:

$$D = \lim_{t\to\infty} \frac{1}{2\Gamma} \langle [\Delta \mathbf{r}(t)]^2 \rangle / t, \quad (4)$$

where Γ is the dimensionality of the space. Time averaging is denoted by $\langle \ldots \rangle$.

The stress in the position of the atom i of the metal film is defined as [7]

$$\sigma_{\alpha\beta}(i) = \frac{\varepsilon}{2a^2 \Omega_i} \sum_{i\neq j}^{k} [-n(a/r_{ij})^{n+2} + cm(1/\sqrt{\rho_i} + 1/\sqrt{\rho_j})(a/r_{ij})^{m+2}] r_{ij}^{\alpha} r_{ij}^{\beta}, \quad (5)$$

where the volume Ω_i related to the individual atom can be associated with that of the Voronoi polyhedron related to the atom i.

The surface roughness (or the arithmetical mean of the profile deviation) was defined as

$$R_a = \frac{1}{N} \sum_{i=1}^{N} |z_i - \bar{z}|, \quad (6)$$

where N is the number of nodes (atoms) on the graphene surface, z_i is the level of the atom i, and $\bar{z}$ is the level of the graphene surface; z_i and $\bar{z}$ are determined at the same instant of time.

RESULTS OF THE CALCULATION

Two configurations of the C–Cu–Ar system (the first of them is related to the first series of ion bombardment and to a time instant of 8 ps, and the second one, to the last fourth series and a time instant of 1.6 ns) are shown in Fig. 1. We chose an Ar_{13} cluster flying out of the central region of the virtual mesh for the first configuration and a cluster beginning its motion from the point located right in the corner for the second one. In Fig. 1a, the first front half of the graphene sheet (the view from the *xoz* plane) was subjected to Ar_{13} cluster bombardment, and the second was not subjected to it. The edge of the graphene sheet in the "zigzag" direction that experienced Ar cluster impacts was curved considerably, as well as the parts of the visible and rear edges in the "armchair" direction, which were hit with Ar clusters. The sheet edges not subjected to ion-beam bombardment retained the ideally straight form. The Cu atoms on the film region "treated" by the ion beam were pressed noticeably against the graphene sheet, while metal atoms on the second film region not subjected to bombardment formed rather loose packing. At the instant of time (8 ps) shown in Fig. 1a, the Ar_{13} cluster closely approaches the Cu film surface. By a time instant of 1.6 ns, i.e., after the target experienced 100 impacts of the Ar_{13} cluster, the graphene sheet was noticeably damaged (Fig. 1b). Either the sheet edges were curved or they had asperities and hollows. The sheet surface became noticeably convex because the central sheet region was protected better by the Cu film than the periphery. A noticeable hollow lay at approximately the middle of the sheet along its entire length at an angle of 15°–17° to the "zigzag" direction. The Cu film above the hollow had a greater thickness than

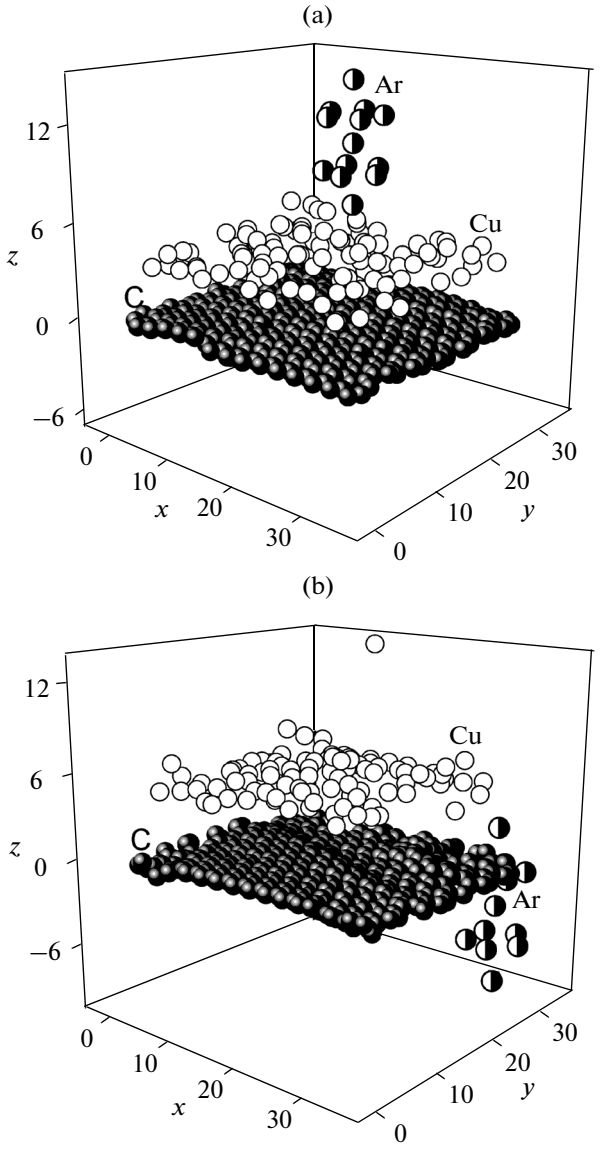

Fig. 1. Configuration of the system consisting of a Cu film on graphene bombarded with Ar_{13} cluster at instants of time: (a) 8 ps and (b) 1.6 ns. The atom coordinates are given in angströms.

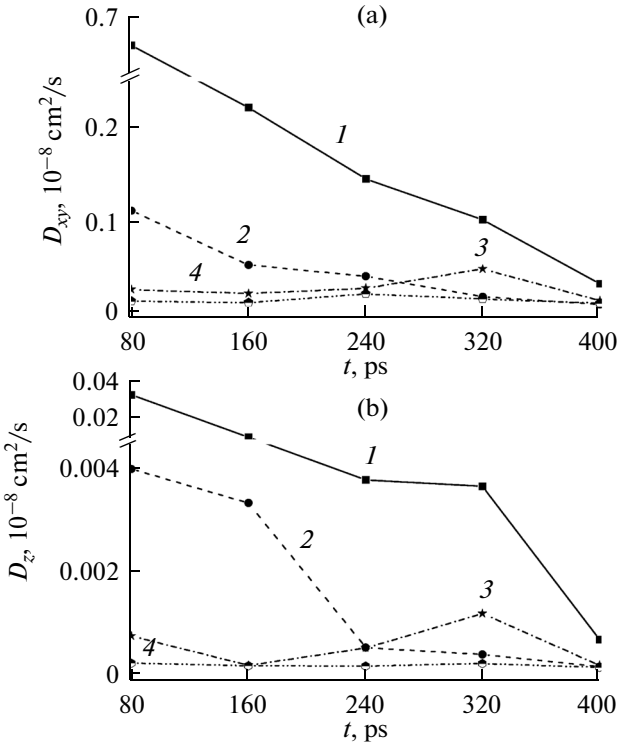

Fig. 2. Components of the self-diffusion coefficient of the Cu film on graphene: (a) *xy* component and (b) *z* component. The numbers stand for the series of ion bombardment.

above the other region of the graphene sheet; i.e., the presence of this defect (the hollow) was due to inhomogeneity of the Cu-film relief. The Cu film became denser and more compact. Cu atoms ejected from the film appeared at the same time. The Ar_{13} cluster reflected from the edges of the metal film and the graphene sheet lost 6 atoms, one of which was near the sheet surface. Thus, bombardment of the target with a low-energy Ar ion beam led to deformation of the graphene sheet and the formation of a dense multilayer Cu film in it.

In view of the specificity of the geometry of the system under study, it is interesting to consider the kinetic properties of its regions separately in the horizontal and vertical directions. Figure 2 shows the horizontal (Fig. 2a) and vertical (Fig. 2b) components of the self-diffusion coefficient of the Cu film for four series of ion-beam bombardment. It can be seen that, in the process of the entire calculation, the Cu atom mobility in the horizontal direction, as a rule, exceeds that in the vertical direction by one order or more. Each new series of target treatment by the low-energy ion beam leads to a decrease in the Cu-atom mobility in the horizontal and vertical directions. The decrease in the mobility was related to the mutual approach of Cu atoms. Within the limits of the first and second series of compaction by Ar_{13} cluster impacts, the Cu atom mobility decreased more gradually in the horizontal directions. The decrease in the metal-atom mobility in the vertical direction for these series of calculations was nonmonotonously. The burst and decrease in the $D_z(t)$ dependence during these stages of bombardment indicate the inhomogeneity of the vertical profile of the metal-film density during the first half of the computer experiment. By the beginning of the third series of impact treatment of the target, the Cu atoms already had a rather close arrangement, which barely differed from the final one in the horizontal plane and the vertical direction for the entire calculation. In the third series of cluster impacts, the $D_{xy}(t)$ and $D_z(t)$ dependences had small minima (at 160 ps) and pronounced maxima (at 320 ps). The presence of these

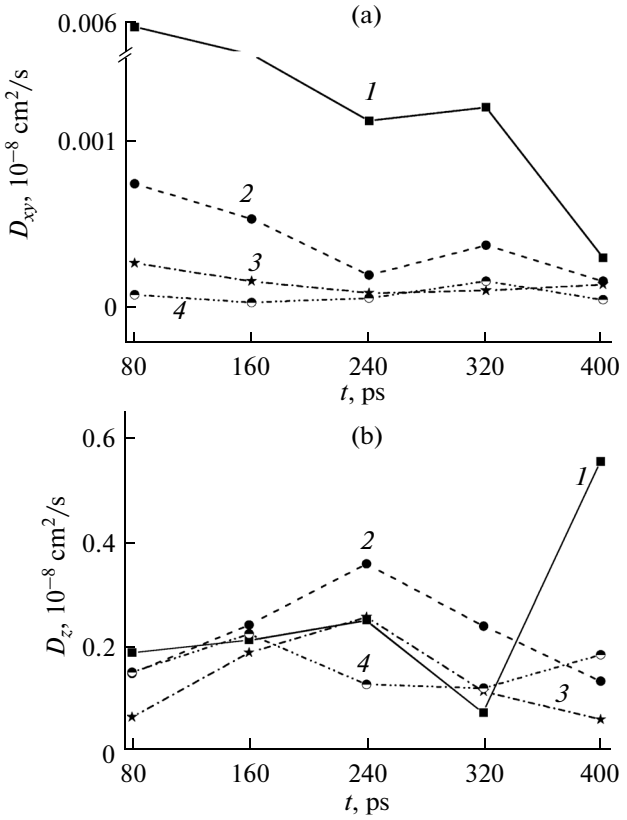

Fig. 3. Components of the self-diffusion coefficient of graphene: (a) *xy* component and (b) *z* component. The numbers stand for the series of ion bombardment.

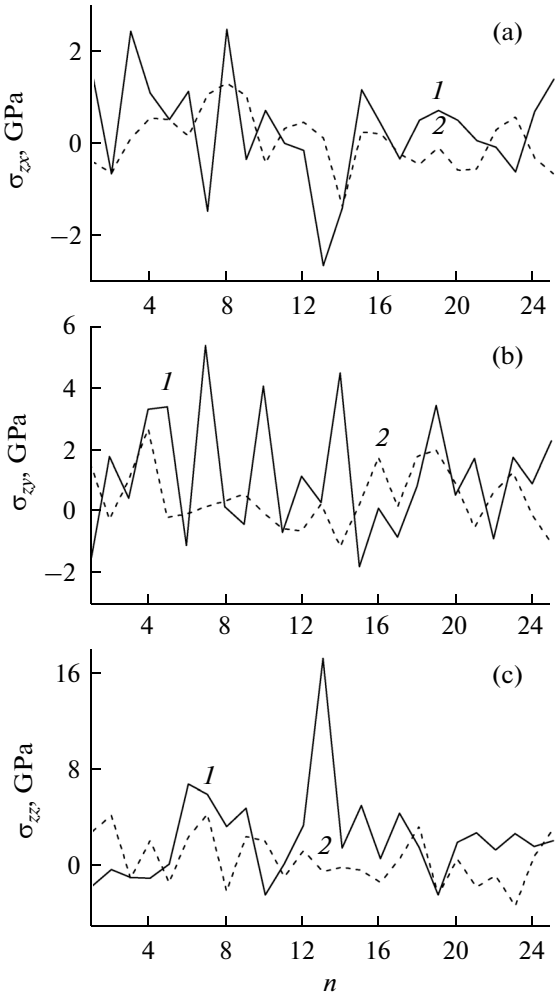

Fig. 4. Stresses appearing in the horizontal plane in the Cu film on graphene: (a) σ_{zx}, (b) σ_{zy}, and (c) σ_{zz} for the series of cluster bombardment: (*1*) the first series and (*2*) the fourth series.

maxima can be related to the ejection of individual atoms from the film. The time D_{xy} and D_z dependences for the two last series of bombardment change slightly at the scale given in Fig. 2.

In the case of bombardment of graphene with an ion beam, the vertical displacements of atoms exceed significantly the horizontal ones (Fig. 3). The four series of cluster impacts with small exceptions are reflected in the behavior of the dependence $D_{xy}(t)$ for graphene in the same way as for the Cu film (Figs. 2a and 3a). The main exception is that a maximum at 320 ps appears during the early stages of impact treatment of the target, i.e., in the dependences $D_{xy}(t)$ (curves *1* and *2*). We note that, at that instant of time, the value of the component D_z of graphene decreases for the same series of cluster bombardment. The mutual compensation of the quantities D_{xy} and D_z means that the C atoms displaced in the vertical direction reveal the possibility of the horizontal motion of other graphene atoms. Unlike the Cu film, the dependences $D_z(t)$ for graphene have a significantly different behavior in series 1–4 of ion-beam bombardment. In this case, during the first 240 ps for series 1–3 and during 160 ps for series 4, an increase in D_z was observed; it was followed by either a temporary (for series 1 and 4) or a constant (for series 2 and 3) decrease. The strongest increase in D_z occurs at 400 ps in series 1. This outburst can be due to the strong vertical displacements of C atoms of the rear "zigzag" edge of the graphene sheet (see Fig. 1).

The values of the components of stresses acting in the horizontal Cu film plane are given in Fig. 4 for series 1 and 4 of ion-beam bombardment. Here, the number n of the cluster impact in the series is plotted on the abscissa axis. The Ar_{13} clusters impacting on the metal film cause not only a strong change in the stresses σ_{zx}, σ_{zy}, and σ_{zz}, but also can change the sign of these stresses. So, for stress σ_{zx}, the sign of this quantity changed 12 times in the first series and eight times in the fourth. The amplitudes of the variations in σ_{zx}, σ_{zy}, and σ_{zz} decrease significantly when passing from the first series of Ar_{13} cluster impacts to the fourth one. Among the curves given in Fig. 4, the function $\sigma_{zz}(n)$ has the maximum stress range, and the function $\sigma_{zx}(n)$, the minimum. The most significant values of

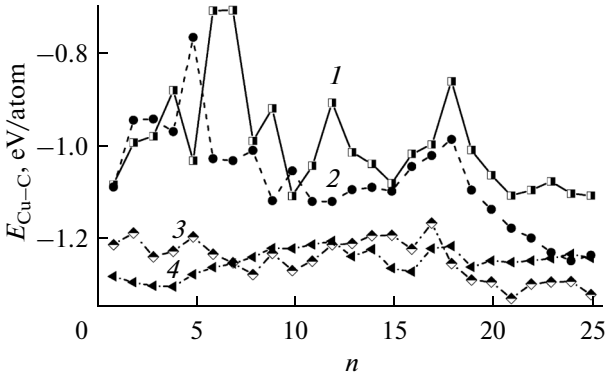

Fig. 5. Cu–graphene interaction energy for four series of ion bombardment. The numbers stand for those of the series.

the stresses σ_{zx} and σ_{zy} appearing in the first series of Ar_{13} cluster impacts are implemented for $n \le 13$, i.e., for the front region (facing the facade) of the film surface (Fig. 1). Among all stresses given in Fig. 4, the largest value (σ_{zz}) appears when the Ar_{13} cluster hit the central region of the Cu film.

The Cu–C interaction energy E_{Cu-C} also experiences strong fluctuations as a function of the number of collisions between the film and the Ar_{13} cluster in each series of ion-beam bombardment (Fig. 5). As a rule, when passing from the first series to the fourth, the energy E_{Cu-C} decreases; i.e., the Cu film is attracted to an increasing extent by the graphene sheet, and the energy fluctuations became less and less pronounced. For a large range of n, a noticeable discontinuity in the energy E_{Cu-C} exists between the two first and two last series of ion-beam bombardment; it disappears at the ends of the series. The energy E_{Cu-C} in the final fourth series is lower than the corresponding energy in the third series only at the beginning and the end of the n range. The opposite pattern is observed in the middle of the range. The minimum energy E_{Cu-C} per unit area, which was obtained in the fourth series of bombardment, was −0.42 eV/Å^2. This value is still higher than the experimental adhesion energy (−0.79 eV/Å^2) of graphene on the Cu substrate [22].

A variation in the averaged structure of the Cu film during ion-beam bombardment of the target can be followed using the radial distribution functions $g_{Cu-Cu}(r)$ shown in Fig. 6. A Cu-film atom that was located at a minimum distance to the center of mass of this film was chosen to construct this spherically symmetric function at each time step. The function $g_{Cu-Cu}(r)$ was constructed for the center corresponding to this atom. Figure 6a shows the radial distribution function determined in such a way for a Cu film not bombarded with an ion beam, and the function $g_{Cu-Cu}(r)$ obtained after all four series of film compaction by Ar_{13} cluster impacts is shown in Fig. 6b. It can be seen that the first three $g_{Cu-Cu}(r)$ peaks determining the average order in

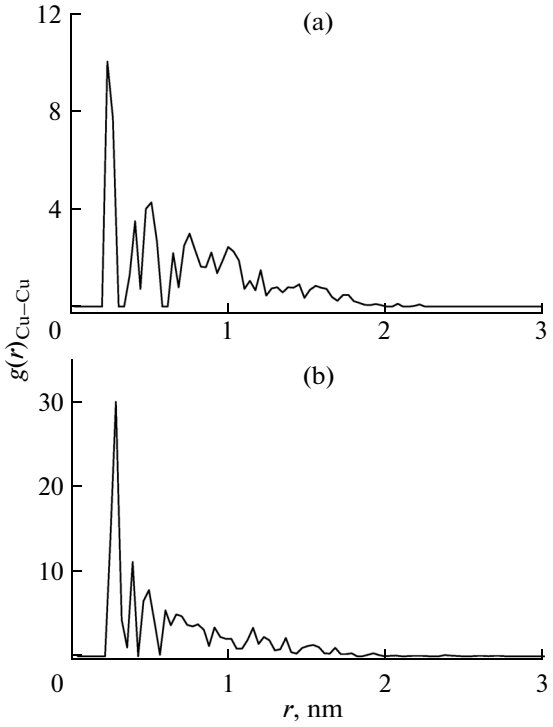

Fig. 6. Radial distribution function for the Cu film on graphene corresponding to the instants of time: (a) 0 ps and (b) 1.6 ns. The instant of time is measured from the emission of the first Ar_{13} cluster in the first series of bombardment.

the film structure have significantly larger intensities after its compaction. In addition, the ratio between the intensities of these $g_{Cu-Cu}(r)$ peaks in this film changes from (2.3 : 0.8 : 1) to (3.8 : 1.4 : 1). Before ion-beam bombardment, these peaks were located at 0.243, 0.417, and 0.522 nm. After ion-beam bombardment of the film, the $g_{Cu-Cu}(r)$ peak positions became determined by distances of 0.278, 0.387, and 0.487 nm, respectively. Because of the increase in the nearest interatomic distances, the metal film became more homogeneous, and formations which were too dense and the large intervals between them disappeared.

In spite of the presence of protection in the form of the Cu film, the effect of Ar_{13} cluster impacts on the graphene-sheet surface turned out to be very perceptible. The change in the graphene-sheet roughness as a function of the number n of cluster impacts is shown in Fig. 7. The three first series of impacts do not lead to an increase in the graphene-surface roughness as the end result. However, after the fourth series, the roughness increased by approximately 60%. Within the limits of each series, the roughness is not a monotonous function of the number n. The strongest R_a fluctuations occur in the first series of ion-beam bombardment. As a matter of fact, the second and third series reproduce the behavior of the function $R_a(n)$ for the first series, but with smaller amplitudes. The fourth series occurs with a smoother oscillating behavior of

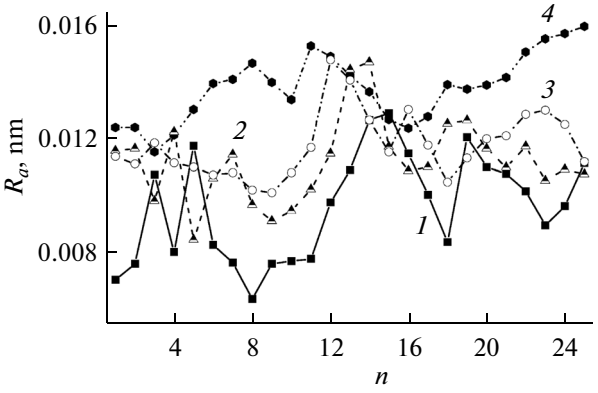

Fig. 7. Graphene surface roughness. The numbers stand for those of the series of ion bombardment.

the function $R_a(n)$ as the roughness increases after the final Ar_{13} cluster impacts. We note that the maximum graphene roughness reached in the fourth series was 500 times smaller than the roughness obtained using the highest 14th class of macroscopic surface treatment.

CONCLUSIONS

Using the MD method, we have studied the ion-beam effect on the kinetic and mechanical properties and the structure of a graphene sheet and a Cu film located on it. The initially loose metal film became more planar and denser under Ar_{13} cluster impacts. The graphene sheet acquired a slightly convex form, and the deformation of its surface reflected the internal surface relief of the Cu film to a certain extent. The horizontal and vertical mobility of Cu and C atoms decreased under Ar_{13} cluster impacts. Both components of Cu atom mobility lost sensitivity to the effect of the ion beam to a significant extent during the fourth series of impacts.

The stresses in the Cu film related to the horizontal plane changed from impact to impact (including a change in sign). Each subsequent series of impacts led to smoothing of the oscillations of these stresses. The absolute maximum for the stress σ_{zz} was attained at the earliest stage of bombardment when the clusters impacted on the central region of the Cu film and the graphene sheet. The Cu-film–graphene interaction energy decreases from one series of Ar_{13} cluster impacts to another. However, approximately half of the impacts make the energy E_{Cu-C} in the fourth series even higher than in the third one. Three coordination spheres reflecting the presence of average order were clearly seen after compaction of the Cu film. Ar_{13} cluster bombardment of the target led to an increase in the graphene-sheet roughness.

ACKNOWLEDGMENTS

The work was supported by the Russian Foundation for Basic Research (grant no. 13-08-00273).

REFERENCES

1. Z. W. Kowalski, Acta Phys. Polon. A **120**, 70 (2011).
2. L. Gilleespie, Laren A. C. Mc, and J. N. Boland, J. Mater. Sci. **6**, 87 (1971).
3. T. Hino, T. Nakai, M. Nishikawa, et al., J. Vac. Sci. Technol. B **24**, 1918 (2006).
4. C. Heck, T. Seki, T. Oosawa, et al., Nucl. Instrum. Methods Phys. Res. B **242**, 140 (2006).
5. J. Tersoff, Phys. Rev. B **37**, 6991 (1988).
6. S. J. Stuart, A. V. Tutein, and J. A. Harrison, J. Chem. Phys. **112**, 6472 (2000).
7. H. Rafii-Tabar, Phys. Rep. **325**, 239 (2000).
8. A. E. Galashev and V. A. Polukhin, Phys. Solid State **55**, 2368 (2013).
9. A. Oluwajobi and X. Chen, Int. J. Automat. Comput. **8**, 326 (2011).
10. A. E. Galashev and V. A. Polukhin, Phys. Solid State **55**, 1733 (2013).
11. Z. Xu and M. J. Buehler, J. Phys.: Condens. Matter **22**, 485301 (2010).
12. S. Jalili, C. Mochani, M. Akhavan, and J. Schofield, Mol. Phys. **110**, 267 (2012).
13. K.-L. Teng, P.-Y. Hsiao, S.-W. Hung, et al., J. Nanosci. Nanotechnol. **8**, 1 (2007).
14. M. C. Moore, N. Kalyanasundaram, J. B. Freund, and H. T. Johnson, Nucl. Instrum. Methods Phys. Res. B **225**, 241 (2004).
15. R. Smith, D. E. Harrison, Jr., and B. J. Garrison, Phys. Rev. B **40**, 93 (1989).
16. A. Delcorte and B. J. Garrison, J. Phys. Chem. B **104**, 6785 (2000).
17. O. Lehtinen, J. Kotakoski, A. V. Krasheninnikov, et al., Phys. Rev. B **81**, 153401 (2010).
18. A. Ito, H. Nakamura, and A. Takayama, J. Phys. Soc. Jpn. **77**, 114602 (2008).
19. A. E. Galashev, J. Surf. Invest.: X-ray, Synchrotron Neutron Tech. **7**, 788 (2013).
20. H. J. C. Berendsen, J. P. M. Postma, W. F. van Gunsteren, et al., J. Chem. Phys. **81**, 3684 (1984).
21. A. E. Galashev, J. Surf. Invest.: X-ray, Synchrotron Neutron Tech. **6**, 623 (2012).
22. S. Das, D. Lahiri, D.-J. Lee, et al., Carbon **59**, 121 (2013).

Translated by L. Kul'man